

Dimensions of the Atlantic–Mediterranean connection that caused the Messinian Salinity Crisis

Dirk Simon ^{*}, Paul Meijer

Department of Earth Sciences, Utrecht University, P.O. Box 80.021, 3508 TA Utrecht, The Netherlands



ARTICLE INFO

Article history:

Received 12 August 2014

Received in revised form 29 January 2015

Accepted 2 February 2015

Available online 12 February 2015

Keywords:

Messinian Salinity Crisis

Modelling

Strait of Gibraltar

Hydraulic control

Gypsum

ABSTRACT

What kind of gateway is needed to cause a salinity crisis? Although several reconstructions of possible Atlantic–Mediterranean gateways are proposed for the late Miocene, so far the gateway that must have existed before the desiccation of the Mediterranean during the Messinian is unknown. This study uses the theory of hydraulic control combined with the effect of bottom friction in order to find out, to first order, the geometrical dimensions of the connection that existed during the Primary Lower Gypsum stage (5.97–5.61 Ma) of the Messinian Salinity Crisis (5.97–5.33 Ma).

The connecting strait is assumed to behave in a similar way as existing straits, such as the Strait of Gibraltar or the Bosphorus. A salinity crisis in an enclosed basin results, when its connection to the open ocean is highly restricted. A strait needs to be relatively shallow, narrow and/or long in order to result in exchange fluxes that are of around 25% or less of the exchange at the Strait of Gibraltar today. Considering the evaporite deposits together with global sea-level variations we estimate the cross section of a strait responsible of the MSC to have a minimum depth of 30–45 m and a maximum width of 0.7–2 km for lengths in the range up to 500 km. These dimensions are consistent with only a few of the Miocene corridors identified. The calculations are extended to explore the implications for sedimentary structures on the corridor floor.

© 2015 Elsevier B.V. All rights reserved.

1. Introduction

Thick sequences dominated by evaporites (up to ~2 km) are present in the Mediterranean Neogene record. Famous gypsum outcrops are located all around the Mediterranean, for example in Spain (Sorbas Basin, Krijgsman et al., 2001) or Italy (Vena del Gesso Basin, Lugli et al., 2010). Halite is evident in the deep basin record (Lofi et al., 2011) and in mines in Sicily. This Messinian Salinity Crisis (MSC, Hsü et al., 1973; Roveri et al., 2014) has been dated, using cyclostratigraphy, to a late Messinian age (5.97–5.33 Ma, Krijgsman et al., 1999a; Manzi et al., 2013). It has been the focus of geologists for about half a century, but the cause of the crisis is still a topic of great debate.

In order to precipitate such evaporites the water salinity of the Mediterranean Sea must have been higher than 130–160 g/kg for gypsum and greater than 350 g/kg for halite. Such extreme salinities in a basin like the Mediterranean are triggered by the interplay between the climate and the connection to the global ocean (Atlantic). This connecting strait is under the influence of tectonics and global sea level changes. The climate parameter that is most important in this context is the water budget (evaporation, precipitation and river input). If the drainage of the Chad basin is excluded, the water budget during the late Miocene is predicted to be of a similar dimension as today (Gladstone et al.,

2007). This leads to the argument that the Atlantic–Mediterranean connection is of great importance in seeking answers about the MSC (Flecker and the MEDGATE Team, in preparation).

Several studies suggest that the Atlantic connection was completely closed during later stages of the MSC in order to desiccate the basin (Roveri et al., 2014). Although alternative interpretations exist (Braga et al., 2006), it is broadly accepted that in the first stage of the crisis, the Primary Lower Gypsum (PLG, 5.97–5.61 Ma) (CIESM, 2008; Manzi et al., 2013), gypsum was deposited all around the margins of the Mediterranean in about 400 ka. For this PLG stage, previous model studies (eg., Topper et al., 2011) show that a connection between the Atlantic and the Mediterranean must have existed in order to supply the Mediterranean with enough evaporites. Fig. 1 summarises some Atlantic–Mediterranean connections that have been reconstructed for the late Miocene (Santisteban and Taberner, 1983). These did not all coexist at the same time, but opened and closed at various times, related to tectonic movements. Notably, Martín et al. (2014) provide paleogeographical maps for specific moments in the evolution of the region. Seaways existed through today's southern Spain (Martín et al., 2009, 2014) and northern Morocco (Krijgsman et al., 1999b). All of these reconstructed corridors are dated to have, probably, closed before the start of the MSC (5.97 Ma). This brings up the question: Where was the gateway that caused the MSC and what did it look like?

In this study the geometry of the gateway is addressed. Strait dynamic theory is implemented in a box model in order to predict the

^{*} Corresponding author.

E-mail address: d.simon@uu.nl (D. Simon).



Fig. 1. Map of the gateway region between the Atlantic and the Mediterranean. Today's coastline is shown by black lines, which indicate the Strait of Gibraltar. The reconstruction of the late Miocene of the region is shown in green (based on Santisteban and Taberner (1983)). Gateways at that time are thought to have cut through the south of Spain (Betic Corridor) and the north of Morocco (Rifian Corridor). The positions of seven corridors are indicated with red dots. For more details about each of these, please consider Table 1 in the Section 5.2 Discussion.

water exchange fluxes through the Atlantic–Mediterranean gateway. Previous model studies (eg., Meijer, 2012; Rohling et al., 2008) considered this connection as a short strait, comparable to Gibraltar, and therefore assume that effects of the length of the gateway can be ignored. Considering the reconstruction of late Miocene gateways (Fig. 1), however, it is clear that the effects of length have played a crucial role (Anati et al., 1977; Pratt, 1986; Garrett, 2004). In order to include the effects of length the effect of friction is implemented which allows us to give predictions about all three gateway dimensions (depth, width and length).

2. Budget considerations

For the PLG stage the sea level of the Mediterranean is thought to be equal to the global level, based on two facts: (1) Facies analyses of the lower gypsum in several basins in the western Mediterranean (Lugli et al., 2008) show strong correlation, which excludes a substantial sea level fall (CIESM, 2008). (2) Moreover, a lowered Mediterranean sea level would not allow for a Mediterranean outflow. Consequently, all the salt flowing in from the Atlantic would be captured within the basin and would raise the salinity beyond gypsum saturation (Meijer and Krijgsman, 2005), for which no evidence is seen in the record. Therefore all the inflowing and outflowing water of the Mediterranean needs to be balanced, as indicated in Fig. 2A. We will sometimes use the term “flux” and sometimes “flow”. The physical meaning of “flux” is the volume transported per unit time. “Flow” refers to water motion in general and is commonly used to describe the velocity of a certain water mass (eg. Section 5.2.1).

The water budget of the Mediterranean is regulated by the balance of evaporation (E), precipitation (P) and river input (R). In order to sustain a basin of enhanced salinity compared to its connected ocean, evaporation must exceed precipitation and river input, leading to a negative water budget. Today's examples of such basins are the Mediterranean, the Red Sea or the Persian Gulf. On the other hand, today's Black Sea, due to a positive water budget, features a lower salinity compared to its connected “ocean”. The Atlantic influx causes the Mediterranean salinity to increase, leading to a density difference between basin and ocean. This density difference establishes an exchange flow, so that Mediterranean waters start outflowing into the Atlantic. Given that

we consider Mediterranean sea level equal to the global one, the five sources and sinks of water of the Mediterranean (Fig. 2) result in the water volume conservation equation:

$$Q_{in} = Q_{out} + e \quad (1)$$

where Q_{in} is the Atlantic influx, Q_{out} is the Mediterranean outflow and $e = E - P - R$ is the effective evaporation (Fig. 2A).

The salt budget depends only on the Atlantic exchange, as evaporation, precipitation and river input are assumed to be fresh water sources and sinks:

$$V \frac{d(S_M)}{dt} = S_A Q_{in} - S_M Q_{out} \quad (2)$$

where the left hand side represents the change of salinity of the Mediterranean basin. V is the volume of the Mediterranean basin and S_M and S_A are the salinities of the Mediterranean and the Atlantic, respectively. The salinity unit (g/kg) we are using in the study is the amount of salt mass (g) dissolved in a certain water mass (kg). Although we are dealing with a high salinity in the Mediterranean, leading to an enhanced density, the difference between its density and that of the Atlantic is still small enough in order to make the Boussinesq approximation. This allows us to set all densities, which are not multiplied by the acceleration of gravity, to an average reference value (Pratt and Whitehead, 2007). Each factor in Eqs. (1) and (2) would be multiplied by this reference and therefore it cancels, which simplifies the mathematics by far, but only has a negligible effect on the final results (Pratt and Whitehead, 2007).

If we consider the steady state case, meaning that the basin salinity reached a certain value at which it stays constant, the left hand side of Eq. (2) will be zero. Meijer (2012) showed that the basin response time to reach steady state after changes in sill depth is of the order of 10 ka (Fig. 6 in Meijer (2012)). This in itself does not conflict with our study, as our aim is to estimate the basin salinity for certain gateway dimensions and boundary conditions for a much longer time scale. As we consider the time span of the PLG stage (~400 ka), phase lags of the order of thousands of years are negligible. A second insight from Meijer (2012) is that due to this lag in the time, depending on the situation, the salinity reached might be slightly lower than the estimated

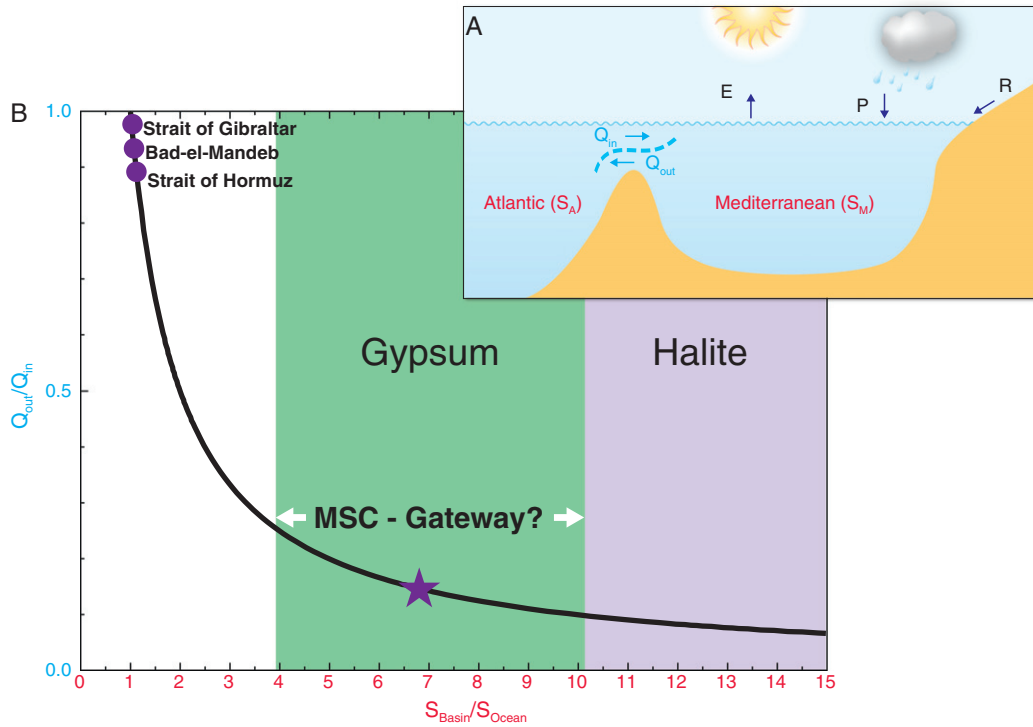


Fig. 2. A) Main water sources and sinks of the Mediterranean basin: Evaporation (E), precipitation (P), river input (R), influx of water from the Atlantic (Q_{in}) and Mediterranean outflux (Q_{out}). B) Eq. (3) leads to this inverse relation between outflux/influx and salinity ratio (S_{basin}/S_{ocean}) (black curve). A great salinity difference can only be sustained with a very low outflux relative to the influx. Three of today's gateways are indicated on the plot (Tsimplis et al., 2006; Johns et al., 2003; Sofianos et al., 2002). Furthermore the regions in which the Mediterranean basin would be at gypsum (green) or halite (purple) saturation are indicated, showing how different a gateway during the PLG (indicated by star and white arrows) must have been compared to today's gateways.

steady state salinity. As our study focuses on first order variations similar to Rohling et al. (2008), such a slight overestimation needs to be kept in mind, but should not greatly affect the conclusions of the study. Therefore we rewrite formula (2) to its rearranged steady state form:

$$\frac{Q_{out}}{Q_{in}} = 1 / \left(\frac{S_M}{S_A} \right). \quad (3)$$

Already this simple relationship indicates that the Atlantic–Mediterranean connection during the PLG stage must have looked different from the gateway today, as illustrated in Fig. 2B.

The curve shows an inverse relationship. To sustain an enhanced salinity (right hand side of plot) the outflux has to be much smaller than the influx. The outflux needs to be less than 25% of the influx of water to reach gypsum saturation and less than 10% to reach halite. This is extremely small compared to today's gateways, where the outflux is close to equalling the influx.

During the PLG stage the Mediterranean must have been of the order of gypsum saturation. Consequently, the outflux must have been of the order of 5–10 times smaller than the influx due to a gateway of quite different dimensions. But, how can basin salinity be related to gateway dimensions instead of fluxes? In the next section we will consider this question by considering strait dynamic theory following the example in previous hydraulic control papers (Meijer, 2012; Rohling et al., 2008; Bryden and Stommel, 1984; Assaf and Hecht, 1974).

3. Theoretical basis

We will consider a gateway between the Atlantic and the Mediterranean with a rectangular cross-section (depth h and width w) and constant length l (Fig. 3). This simplified geometry allows us to study the importance of each strait dimension in isolation.

3.1. The momentum equation

In order to relate the strait dimensions to the flow rates we consider the momentum equations for each layer (see Appendix A for details). As there are many different forces that affect the water flow, it is necessary to weigh their importance.

In ocean straits the horizontal length scale is much greater than the vertical one, which enables us to use the shallow-water equations. These are derived by applying the long-wave approximation to the Navier–Stokes equations by integrating along the depth of the fluid, which allows for a simplified mathematical formulation (Pratt and Whitehead, 2007). Following Assaf and Hecht (1974) and Pratt and Whitehead (2007) the conservation of momentum between the bottom and top layer in our gateway can be written as:

$$u_{out} \frac{du_{out}}{dx} - u_{in} \frac{du_{in}}{dx} = g' \frac{dh_{in}}{dx} + C_D \frac{u_{out}^2}{h_{out}} \quad (4)$$

where u_{out} , u_{in} and h_{out} , h_{in} are the outflow and inflow velocities and layer depths, respectively. x stands for the direction along the corridor, while C_D is the bottom friction coefficient and g' is the reduced gravity. This momentum equation is for the case of steady flow, as it is common practise in these kinds of problems (eg. (Meijer, 2012; Pratt, 1986; Assaf and Hecht, 1974)).

The left hand side of Eq. (4) represents the difference in inertia of the two water layers. If $Q_{in} \approx Q_{out}$, this difference can be approximated to be very small, which led Anati et al. (1977) to ignore it. In the MSC case, the influx must have been quite different from the outflux, making it important to retain the term.

The first term on the right hand side represents the pressure gradient between the Atlantic and the Mediterranean. This gradient is due

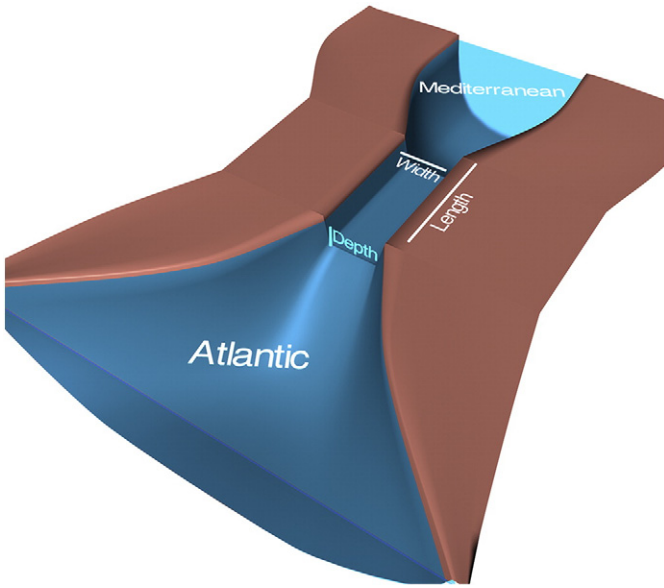


Fig. 3. The simplified gateway between the Atlantic and the Mediterranean, we consider it rectangular in shape and of constant width w , depth h and length l .

to the density difference of the two basins/layers. It is hidden within the reduced gravity term:

$$g' = g \frac{\Delta\rho}{\rho_M} = g \frac{\rho_M - \rho_A}{\rho_M}. \quad (5)$$

In order to connect this relation to the salinity difference between basin and the ocean, an equation of state is needed. Following Bryden and Stommel (1984) we use:

$$\rho_M = \rho_A + \beta(S_M - S_A) \quad (6)$$

where $\beta = 0.77(\text{kg/m}^3)/(\text{g/kg})$ is the haline contraction coefficient. In view of our emphasis on elevated salinity the effect on the density of temperature and pressure is ignored (see Topper et al. (2011) for a discussion). Both Warren (2006) and Feistel (2008) reported density of seawater to increase essentially linearly with salinity up to conditions close to gypsum saturation (starting at 130 g/kg) which justifies our use of a constant coefficient (Meijer, 2012).

The second term on the right hand side of Eq. (4) is the friction term. It concerns the bottom friction, meaning the retardation force on the bottom layer due to the shear between water flowing in the bottom layer and the gateway floor. It is crucial to consider this term here, as it will allow us to account for the length of the gateway, rather than just the cross section (Meijer, 2012; Rohling et al., 2008). The bottom friction coefficient depends on parameters like the channel bottom topography and the sediments present (Te Chow, 1959). As we have no control on what these might have been in the last corridor before the MSC desiccation, we will use a range of values of today's gateways 0.005 to 0.012 (Zaremba et al., 2003; Gu and Lawrence, 2001; Pratt, 1984). The friction along the other surfaces or interfaces of the gateway is not taken into consideration. Side wall friction can generally be ignored if the hydraulic radius ($w * h/(w + 2h)$) is about equal to h , as it is valid for this study (Officer et al., 1976). Surface friction is assumed to have an effect on the asymmetry of the interface between the layers, but a negligible effect on the exchange flux (Gu and Lawrence, 2005) and will therefore not be considered in this study. Assaf and Hecht (1974), Gu and Lawrence (2005) or Zaremba et al. (2003) include the effect of interfacial friction between the two layers. This would also be an option in this study. We decided, though, not to include the effect

of interfacial friction in our theory for two reasons: (1) Due to interfacial friction another friction factor needs to be considered. Not many measurements from today's gateways exist regarding this friction factor and it seems generally hard to predict (Zhu and Lawrence, 2000). (2) Already by including the bottom friction the importance of the length and friction can be analysed (Pratt and Whitehead, 2007). A further effect linked to the interface, that we ignore, is the interfacial mixing. This mixing between the counterflowing layers is known to occur, but it is not well understood how it affects the exchange flow [Ivey, 2002]. Özsoy et al. (2001) study interfacial mixing for the case of the Bosphorus. In general mixing between the two layers might decrease the density difference between them, this would lead to a lower reduced gravity in Eq. (5) and thus correspond to a weaker exchange between the Atlantic and the Mediterranean.

The Coriolis effect will have a greater effect on the momentum balance with increasing width of the gateway. Generally, the Coriolis force can be neglected if the width of the gateway is smaller than the Rossby radius $R = \frac{\sqrt{g'h}}{f}$, where h is the total gateway depth and $f (= 8.5 * 10^{-5} \text{ s}^{-1})$ is the Coriolis parameter for the appropriate latitude (Whitehead, 1998). As our focus is on gateways of width of 10 km or less, the simplification is justified. In order to relate Eq. (4) to the water and salt conservation equation in Section 2, the velocities need to be changed to water fluxes, using $Q_{out} = u_{out} * h_{out} * w$ for the bottom layer and likewise for the top layer. After rearrangement the resulting relation (see Appendix A) is:

$$\frac{Q_{in}^2}{h_{in}^3} + \frac{Q_{out}^2}{h_{out}^3} (1 + F) = w^2 g' \quad (7)$$

where w is the corridor width and $F = \frac{C_D}{\frac{dh_{out}}{dx}}$ is the factor that brings in the effect of friction. If F is set to zero, which effectively equals a "frictionless" or "lengthless" gateway, Eq. (7) becomes the well known hydraulic control equation (e.g., Bryden and Stommel (1984)).

3.2. Computing the interface position and basin salinity

Eq. (7) relates the water fluxes to the strait dimensions. By combining it with the conservation of salt and water (see Appendix A), this turns into Eq. (8), that can be used to predict the expected average basin salinity for specific gateway dimensions and effective evaporation across the basin. For depth, width and length we will explore a range of values in the next section. Evaporation will be set according to previous climate studies (eg. Gladstone et al. (2007), which is also close to today's value Mariotti et al. (2002)) and will be further discussed in Section 5.

$$\frac{1}{\left(1 - \frac{S_A}{S_M}\right)^2 (1-f)^3} + \frac{(1+F)}{\left(\frac{S_M}{S_A} - 1\right)^2 f^3} = BC \frac{S_M - S_A}{\rho_A + \beta(S_M - S_A)} \quad (8)$$

where

$$f = h_{out}/h \quad \text{and} \quad BC = \frac{h^3 w^2 g \beta}{e^2}. \quad (9)$$

There are two further variables that need to be set: (1) the average interface gradient ($\frac{dh_{out}}{dx}$ in F) of the interface of the two water layers and (2) the interface height $f = h_{out}/h$.

We let the interface along the channel vary linearly, so that $\frac{dh_{out}}{dx} \approx \frac{h}{l}$. This is a simplification, but based on the following reasoning we concluded that it is a valid approximation given the first order nature of our analysis. Anati et al. (1977) compared laboratory experiments to theory that is also based on Eq. (4), but by ignoring the inertia term on the left hand side. They found that the results came to reasonable agreement. Nevertheless, Gu and Lawrence (2005) showed that the

interface along the channel can be approximated to being linear in the middle of the channel (part in our focus), but is curved towards the ends. Gu and Lawrence (2005) compared their results to those of Anati et al. (1977) indicating that the flux is slightly overestimated for short channels and slightly underestimated for long channels in the Anati study, but in a range that is acceptable in our first order model set-up, which focuses on the average exchange flux through the corridor instead of on the interface. One major improvement of our model, compared to that of Anati et al. (1977) is the inclusion of the inertia of the two layers flowing which will further decrease the uncertainty and give a realistic result (see Pratt and Whitehead (2007) for further discussion). Moreover, the interface gradient always occurs in combination with the bottom friction coefficient C_D in the term F . The variation of C_D will already give a range of answers, which will make effect of variation in interface gradient relatively small.

Another important variable to be considered is the interface depth $f = h_{out}/h$. Whereas Meijer (2012) considered many different interface depths in order to study how it affects the exchange, in this study we will focus on a single one: that of the maximal exchange solution [Farmer and Armi, 1986, 1988 and Armi and Farmer, 1987; see also Dalziel, 1992]. The maximal exchange solution provides, for a given gateway geometry, the lowest possible basin salinity. If the interface lies below or above of where the maximal exchange requirement places it, the exchange is less than maximal and basin salinity higher. The same holds true if we were to include interface friction or the Coriolis force: these also reduce strait efficiency and would yield higher salinity for a given strait geometry. Thus, if our question is which strait geometry is needed to reach a specific elevated basin salinity (for instance, the gypsum saturation value), our analysis provides us with the minimum cross section and the maximum length of the responsible gateway. The actual gateway may have been deeper, wider or shorter, but only if there were other factors at play reducing its efficiency.

The method to find the interface depth for maximal exchange is described in Stommel and Farmer (1953) and Bryden and Stommel (1984). Although we follow the same reasoning, our Eq. (8) looks slightly different from Eq. (5) in Bryden and Stommel (1984) because friction is included. Eq. (8) is plotted in Fig. 4 for a specific case. The y-axis indicates the depth of the non-dimensionalised channel depth at the centre of the channel and the x-axis is the expected salinity of the lower layer, which in our case equals Mediterranean salinity. The graph shows that in this case for salinities lower than about 95 g/kg there is no solution

to Eq. (8) while above this value there are always 2 possible interface positions that would lead to the same basin salinity. Here we, basically, present the same idea as Fig. 2 in Bryden and Stommel (1984), but in a way that allows us to compare directly the interface position with basin salinity. The turning point on the graph is the only point where a unique solution exists, which equates to the maximal exchange solution. Using differential techniques it is possible to find the exact value at the turning point for any kind of channel dimensions, Atlantic salinity and effective evaporation.

4. Model results

Eqs. (8) and (3) allow us to calculate Mediterranean salinity and the exchange fluxes in the gateway for given gateway dimensions. The overall result is that in order to restrict a basin strong enough to cause highly saline waters, the gateway connecting it to the global ocean needs to be relatively long, shallow and/or narrow. This intuitive result is quantified below.

4.1. Cross section variations

The effect of variations in gateway cross section on basin salinity and exchange flux is illustrated in Fig. 5. Depth and width are considered separately, although their general behaviour is similar, as already studied in Meijer (2012) for short gateways.

For depth approaching 150 m and beyond and for width exceeding 5 km the curves show minor variations in the exchange flux ratio and basin salinity. Such “large” gateway dimensions apply to straits like the present Strait of Gibraltar (depth ~300 m and width ~14 km). As seen in Fig. 2, the salinity difference between the Atlantic and the Mediterranean is indeed very low today (about 2 g/kg) and the outflux almost matches the influx.

Shallower (less than 150 m) and narrower (less than 5 km) gateways show much stronger variations in response to changes in depth or width. Whereas the exchange flux strongly decreases towards a state in which the outflux is much smaller than the influx, the basin salinity increases in large steps with small decrease in depth or width. This highly nonlinear trend will have a major impact on the basin salinity when the gateway is already narrow or shallow. If such a shallow gateway is influenced by global sea level variations the salinity of the basin may change dramatically. This has already been considered by Rohling et al. (2008) and will be reconsidered in Section 4.3. The effect of length and friction can also be seen in Fig. 5, as the variation of these two factors determines the thickness of each coloured band. Minimum salinity and maximum exchange ratio refer to the frictionless case and maximum salinity and minimum flux corresponds to a bottom friction coefficient of $C_D = 0.012$ and a length of $l = 1000$ km.

4.2. Length variations

The effect of gateway length is further demonstrated in Fig. 6. The general trend indicates that the longer the gateway, the greater the restriction and therefore the higher the basin salinity. The reason for this is that the bottom friction slows down the bottom current, which allows less water to flow out. Because of the conservation of water (Eq. (1)), if less water flows out, less water flows into the Mediterranean. The resulting steady state has a lower exchange flux ratio (more restriction) and results in a higher basin salinity.

In general it can be seen that for shorter gateways (less than 400 km) the salinity increases and flux decreases in a more rapid and nonlinear way with increasing length. This levels out into a roughly linear increasing salinity and decreasing flux for longer gateways. The deeper or wider a gateway is, the less important the effect of length, as seen in Fig. 6 (top right). With width equal to 5 km the salinity only varies by about 10 g/kg for the 100 m deep corridor and about 30 g/kg for the 50 m deep corridor. Although these variations are large in a normal

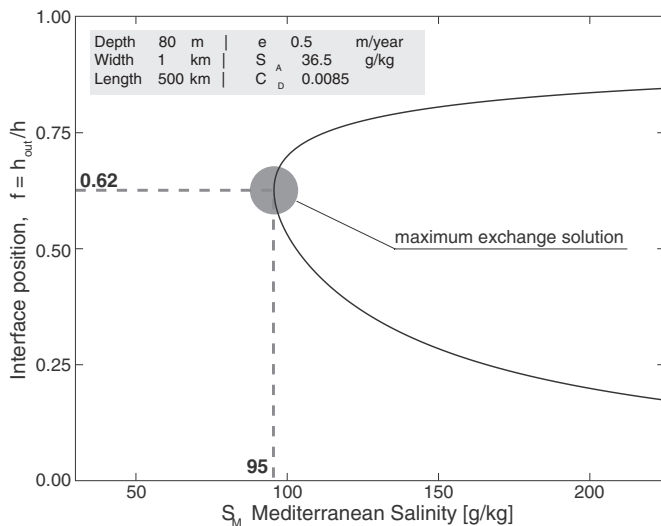


Fig. 4. Plot of interface depth $f = h_{out}/h$ and Mediterranean salinity S_M , using Eq. (8). There is only one salinity that has a single solution for the interface. This salinity is the solution for maximum exchange, as indicated by the grey circle and the dashed lines. The parameters used for this example are indicated in the box.

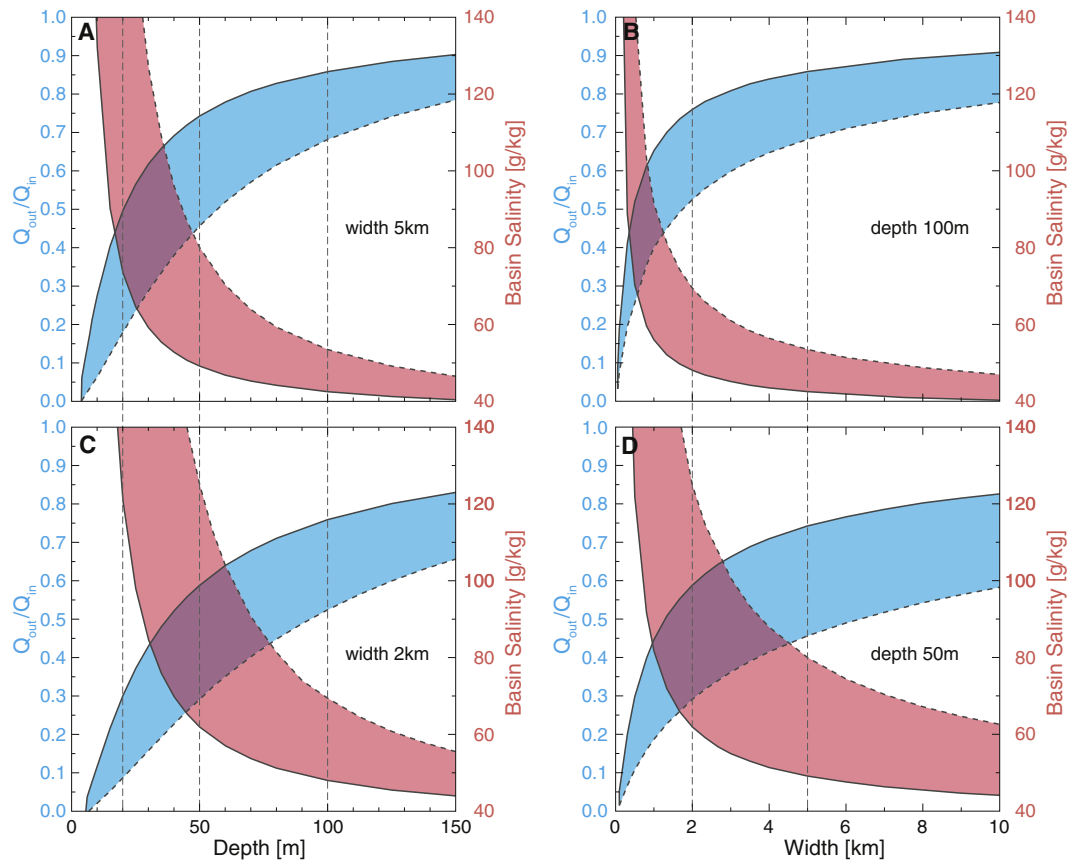


Fig. 5. Panels show basin salinity (red) and exchange flux ratio (blue) and how they vary for different gateway depth (left hand side) and different width (right hand side). Each variation is presented by a range (coloured area) due to the change in length and friction factors used. The minimum salinity or maximum flux ratio always refers to the case of no friction or effectively no length ($F = 0$). This is indicated by the solid black line at the bottom of the red region and top of the blue region. The maximum salinity or minimum flux ratio always refers to $F = C_D * l/h$, where the maximum C_D is 0.012 and we let the length l vary up to 1000 km at first. This is indicated by the dashed black line at the top of the red region and bottom of the blue region. The role of length in setting the range is demonstrated in Fig. 6 for the cases (depth 20 m, 50 m and 100 m and width 2 km and 5 km) indicated with the horizontal dashed black lines.

oceanographic sense, they are minor against the background of a basin leading into gypsum and, even, halite saturation. Therefore for these deep and wide corridors the effect of length and friction is minor in the context of the MSC. On the other hand, for shallower or narrower gateways as shown in Fig. 6 (left and bottom) the salinity variation due to length can be much more severe and may actually control whether the basin reaches, for example, gypsum saturation.

4.3. Gateway dimensions that lead to gypsum saturation in the Mediterranean

The maximum possible length a gateway connecting the Atlantic to the Mediterranean can have had is around 500 km, because this is the maximum distance through Spain or Morocco. If we set the gateway to this length, it is possible to reorganise the above results in order to show what kind of cross section is needed to reach gypsum saturation in the basin. The result is shown in Fig. 7. It shows, again, that a greater cross section will lead to a less saline basin and a smaller cross section to a more saline basin. Any cross section picked in the green region will lead to a basin of gypsum saturation. This might, for example, be a gateway of 10 km width and 10 m depth or a gateway of 800 m width and 70 m depth.

This still allows for many different cross sections for a certain gateway length, therefore here we need a method for limiting these results in order to get a first order estimate of the gateway dimensions that led to the MSC. Our approach is similar to Rohling et al. (2008), but in reverse.

The PLG phase of the MSC lasted from 5.97 Ma to 5.6 Ma (Manzi et al., 2013). During this ~400 ka period, layers of gypsum were

deposited in various locations around the margins of the Mediterranean (Krijgsman et al., 1999a). The gypsum occurs in regular alternations that have been tuned to be caused by climate cycles due to precession of the Earth (Krijgsman et al., 2001). What is not seen is an expression of obliquity-controlled sea level variations (Krijgsman et al., 1999a; Hilgen et al., 2007). Apparently, the gateway dimensions were such that changing global sea level did not cause basin salinity to either pass below, or reach beyond, the gypsum saturation field.

The global sea level is thought to have varied by around 10 m before the start of the MSC (6.14 Ma) and up to an amplitude of around 30 m at 5.26 Ma (Aharon et al., 1993), timescale of Hilgen (1991)). Further evidence for these fluctuations was given by Braga and Martín (1996), estimating sea level changes of the order of tens of metres in the Sorbas basin. These estimates of 10–30 m sea-level variations are consistent with the amplitude of the benthic $\delta^{18}\text{O}$ changes in Site 982 (Hodell et al., 2001). Therefore we assume that a sea level variation of an amplitude of around 20 m need to be able to sustain a Mediterranean basin at gypsum saturation.

We can now return to Fig. 7 and pick the gateway that will allow for these sea level changes, but still satisfies the gypsum saturation. For a gateway of 500 km in length the minimum depth is around 30 m and the maximum width is around 1.5 km. By repeating this thought process for various lengths of up to 500 km it is possible to find a range of the gateway cross sections that existed during the PLG stage of the MSC. From this we can conclude that the cross section during that time had a minimum depth of about 30–45 m and a maximum width of about 0.7–2 km.

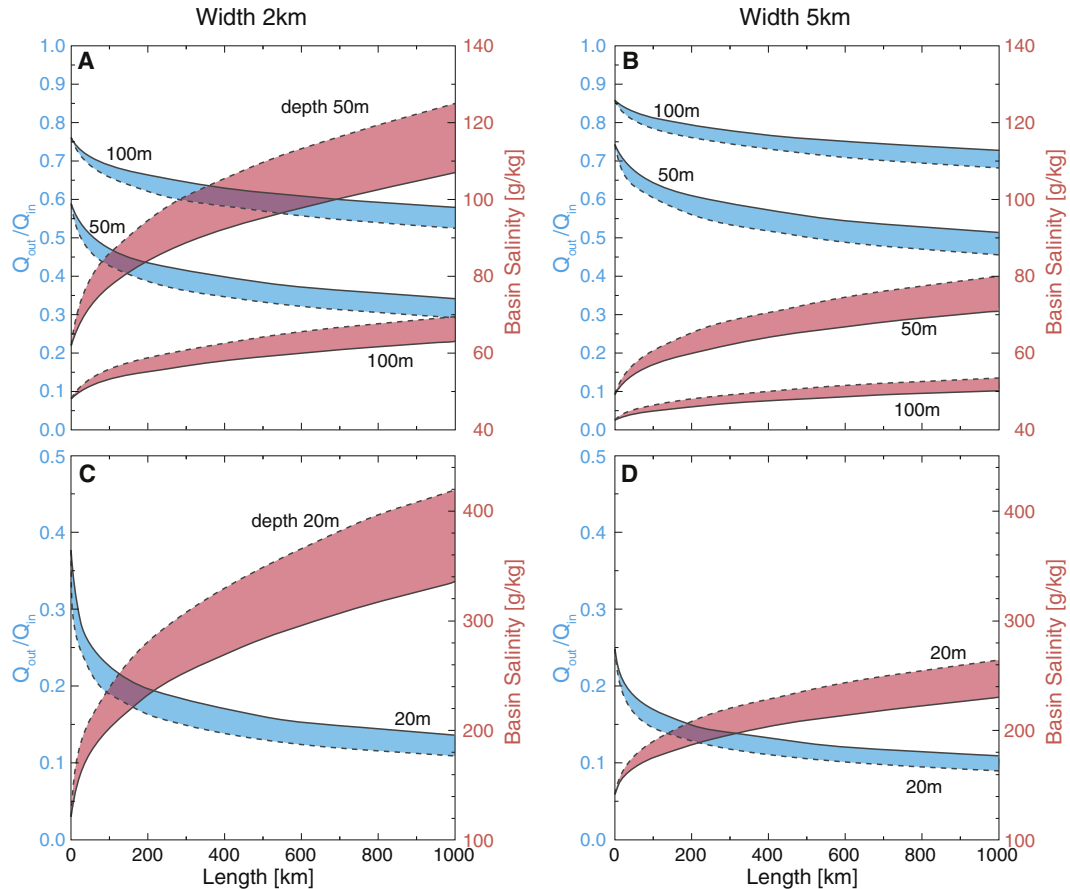


Fig. 6. Plots of variations in water flux ratio and basin salinity with gateway length. The variations shown are the ones indicated by the horizontal dashed lines in Fig. 5. Bottom friction coefficients are set to the range of 0.005–0.012. The minimum salinity or maximum flux ratio always refers to the case of $C_D = 0.005$, which is indicated by the solid black line at the bottom of the red region and top of the blue region. The maximum salinity or minimum flux ratio always refers to $C_D = 0.012$, which is indicated by the dashed black line at the top of the red region and bottom of the blue region. Top: Gateway depths are 50 m and 100 m for gateway width of 2 km (left side) and 5 km (right side). Bottom: Gateway depth of 20 m, due to this very shallow depth different salinity and flux ratio scales had to be chosen.

5. Discussion

In this study, the theory of hydraulic control with the inclusion of bottom friction is used in order to relate the exchange flux and basin salinity to the strait dimensions. Here we evaluate some of the assumptions and the effect on the model results of specific variables. We also consider our results in the light of previous work and explore their implications.

5.1. Model evaluation

5.1.1. Response to climate change

“Climate” in our model is represented by the effective evaporation $e = E - P - R$. It is set to a value that lets 0.5 m of Mediterranean water at the surface disappear within a year, which is based on Gladstone et al. (2007). Gladstone et al. (2007) exclude the drainage of the Chad basin, which could lead to the increase in river input and therefore to a less negative, or even positive water budget.

Already by considering the water and salt conservation (Eqs. (1) and (3)) it is clear that an increase in e will lower the flux ratio and a decrease in e will increase the flux ratio. Fig. 8 shows how our model responds to different values of e for a given gateway. Basin salinity basically changes linearly. Meijer (2012) considered some variation of effective evaporation in his model. Fig. 4c in Meijer (2012) illustrates that an effective evaporation variation of 0.50 ± 0.25 m/year will lead to a salinity variation of about ± 30 g/kg. This is consistent with what we predict for the frictionless case, keeping in mind that the interface

position in Meijer (2012) is constant for each case, but ours is always the maximal exchange solution. When friction is included the linear trend stays, but the salinity change is more extreme for a given e variation. For an effective evaporation variation of 0.50 ± 0.25 m/year the salinity variation is about ± 60 g/kg. Such a linear trend makes it straightforward to extrapolate Figs. 5 and 6 for different effective evaporation values.

5.1.2. Response to interface position

For our model we choose to stay within the overmixing limit (Stommel and Farmer, 1953; Bryden and Stommel, 1984), which sets the interface to its lowest energetic state. This is the state that will ensure the maximal exchange between the two water masses. To note is that the bottom friction slows down the bottom current and therefore causes the interface to sit higher than it is expected without friction. Different points on the curve of Fig. 4 indicate how the interface changes if the system would not be at maximal exchange. Meijer (2012) considers different interface positions for the frictionless hydraulic control case. With friction we notice that for less restricted gateways small changes in the interface position will hardly affect the basin salinity. The greater the restriction, however, the more sensitive will the predicted salinity change with interface position. Therefore it is also important to consider the factors that control, whether the system can be considered to be in maximal exchange. Armi and Farmer (1987) summarise the main features that need to hold in order to consider an exchange to be maximal. This comes down to the requirement that the flow through the strait is bounded by supercritical flows at each side. Whether a flow is defined

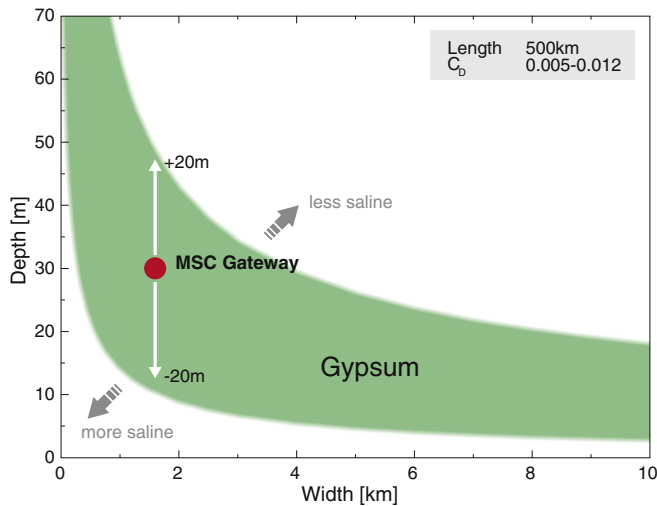


Fig. 7. The range of combinations of depth and width of a 500 km long gateway, that will cause gypsum saturation in the Mediterranean. The bottom friction coefficient is in the range $C_b = 0.005\text{--}0.012$. Moreover the sea level variation of an amplitude of 20 m are indicated with the a gateway at its minimum depth.

to be supercritical depends on the combined Froude number, if that is larger than unity, the flow is said to be supercritical. On the Atlantic side of our channel the bottom layer becomes very shallow and the flow velocities high, therefore the combined Froude number will easily reach a supercritical stage. On the Mediterranean side, the depth of the top layer start tending towards zero, as the flow enters the basin, which also set the flow in a supercritical stage. This indicates to us that it is a reasonable assumption to take the flow to be maximal. This requirement always holds, even for unsteady cases or when friction is considered (Armi and Farmer, 1987).

5.1.3. Further restricting effects

Our study focuses on gateways of constant depth, width and length. Fig. 1 shows reconstructed gateways that seem more complex. The more complex the geometry of these gateways is, the more additional effects on the exchange flux and therefore on the basin salinity will come into play. Potential complexities are channels with many bends and curves, that could resemble a meandering river, islands sitting within a channel, multiple channels, or varying cross section (depth and width). We speculate that these effects could lead to: (1) An increased effective length of the channel, leading to further restriction, as indicated in Fig. 6. (2) An effectively smaller cross section, due to changing depth and width, which would also lead to more restriction, as demonstrated in Fig. 5. (3) More turbulence at the sides or bottom, which would add an extra retardation effect. Once more control is available about the connection that existed during the PLG stage from field and proxy studies, it becomes meaningful to study these effects in more detail. For example with a regional ocean general circulation model (see de la Vara Fernández et al. (in review)).

Interfacial friction will also further restrict the exchange, in a way that is expected to be similar to the role of bottom friction. That is, less important for deeper and shorter gateways and potentially more important for shallower and longer ones. Zhu and Lawrence (2000) conclude that the friction factor associated with interfacial friction is not easy to measure or predict accurately, because of its dependence on turbulence between the flows. Although it is thus hard to say to which extent interfacial friction will affect the exchange, it is clear that it will allow for gateway dimensions that can be slightly deeper, wider or shorter in order to reach the same salinity in the basin. Mixing across the interface between the two flowing layers would have a similar effect (see Theory Section 3). Therefore the greater the interfacial mixing, the lower the exchange of water between the ocean and the basin. This

would lead to higher basin salinities, just as decreasing gateway depth or width or increasing its length.

A final factor of which the effect is likely to always remain highly uncertain, is the occurrence of tides. Our velocities may be thought of as representing the mean state, averaged over multiple tidal cycles, only to the extent that tides impose a linear oscillation on the exchange flows. For specific channel geometries resonance may occur (Officer et al., 1976) and the effect may be nonlinear. To tackle this uncertainty in a meaningful way would seem to require knowledge regarding channel geometry much more precise than we have available.

5.2. Relevance of the results

5.2.1. Implications for sedimentary bed forms within the gateway

Although, so far, we focussed on water transports, our results can also be expressed in terms of the mean velocities of flow in each of the two layers (using $Q = u * h * w$, where u is the layer velocity). The rate of flow in the bottom layer is of particular interest because it is related to the sedimentation, transport and/or erosion that occurs on the gateway floor. This potentially provides another link between the model and geological observations.

Here we focus on a gateway of channel dimensions with depth of 30 m, width of 1.5 km and length of 500 km. For an effective evaporation, that would remove 0.5 m of water from the whole surface of the Mediterranean per year, this gateway would cause an exchange flux that would lead to gypsum saturation in the basin, as shown in the results (Section 4.3). Fig. 9 illustrates this gateway with the two water layers indicated. The mean outflow velocity along the channel is calculated from modelled outflux. The depth of the bottom layer varies along the channel. The interface is taken to be linearly varying along the channel, leading to a relative high flow velocity close to the Atlantic and a much lower one on the Mediterranean side, with a gradual variation in between. This does not give the exact interface depth at a certain channel position, but provides values for mean velocity that are of the right order. Fig. 9 also shows how the mean flow velocity varies for a certain position along the corridor. Because the velocities are plotted with a log-scale it is straightforward to link the velocities to the bed form diagram on the right. This diagram is simplified from experimental/laboratory studies of steady unidirectional water flows of rivers, by Boguchwal and Southard (1990) and Ashley et al. (1990). Although there are several different bed form diagrams in use with various velocities or shear stresses studied, we decided to use this one, as according to Leeder (1999) it is the most simple representation, which is in accordance with our aim to gain first order insights. It has been used in numerous of studies, although it is important to keep in mind that the scaling from laboratory experiments to natural environments and

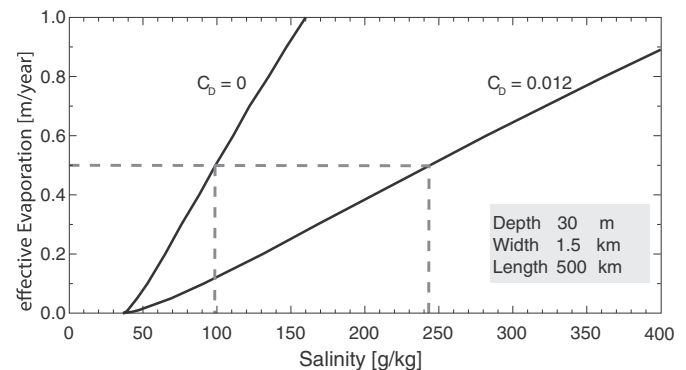


Fig. 8. The effect of the change in effective evaporation on the basin salinity for a gateway of depth of 30 m, width of 1.5 km and length of 500 km for the zero friction case and the maximal friction case. The dashed line indicates the salinity values for this gateway example.

the use of a mean velocity can cause uncertainties (Leeder, 1999; Kostaschuk and Villard, 1996).

Fig. 9 indicates that on the Mediterranean side for finer grains we should expect ripples and no motion for coarser grains. The further away from the Mediterranean and the closer to the Atlantic, the cross section of the bottom layer decreases and the corresponding increase of the average flow velocity would lead to dunes and anti-dunes.

This first look at the problem already provides important insight. Although intuitively one might expect that a very restricted gateway would be associated with high flow rates and therefore would perhaps be dominated by erosion, here we show that the velocities would correspond to “normal”, well known sedimentary structures that should be able to be recognised in the field. Betzler et al. (2006) and Martin et al. (2001) describe cross-bedded strata within the Guadix basin and the Guadalhorce corridor. It is important to stress, though, that these two studies consider sediments of ages older than 7.8 Ma and 6.3 Ma, respectively, which relate to earlier stages of the gateway we are looking for. We are here considering the corridor that must have existed during the first stage (5.97–5.6 Ma) of the MSC (Topper et al., 2011; Roveri et al., 2014).

5.2.2. Which gateway was the last existing one?

The purpose of this study is to estimate the dimensional limits of the Atlantic–Mediterranean connection during the PLG stage. We know that a connection must have existed (Topper et al., 2011), but where the connection was, is still to be determined. Fig. 1 shows several of the Atlantic–Mediterranean corridors reconstructed for late Miocene time. They did not all coexist at the same time but opened and closed through time related to tectonic movements. The reconstructions are based on connecting sediment patches of equal ages. Commonly, closing ages are determined from sedimentary successions that document a change from marine to continental conditions (eg., Krijgsman et al., 1999b). Most of the corridors are associated with an unconformity (eg., Hüsing et al., 2010 or Krijgsman et al., 1999b). From the outcrop alone it is not possible to determine whether the unconformity is non-depositional such that the youngest marine sediments are indicative of the timing of the last marine connection, or is erosional so that exchange persisted, but the record of it has been removed. An additional source of uncertainty regarding the age of closure comes from the

question whether the end of marine sedimentation in a basin adjacent to a corridor is indicative of the time of closure of the corridor itself (see, for example for the Granada basin, Martín et al. (1984) and Garca-Veigas et al. (2013, 2015) versus Corbí et al. (2012)).

A new approach to constraining the timing of closure is the use of isotope water mass tracers measured in continuous Atlantic records. For the Rifian corridors (from the section Ain el Beida in northwest Morocco), Ivanovic et al. (2013) suggest that at least a component of the age gap is generated by erosion. Likewise, for the Guadalhorce Corridor (Betics) an end of the Mediterranean outflow can be dated to 6.18 Ma (Pérez-Asensio et al., 2012). In an attempt to contribute to this discussion, we will look at the problem from a different angle, considering the dimensions only, irrespectively of the proposed closure time. The most important corridors are summarised in Table 1, together with their estimates of width and length. Corridor width (Table 1, column 3) represents a minimum, as the edges of the seaways may have been removed by erosion. Corridor length (Table 1, column 4) is a matter of definition. We took the length of the corridors to be the length at which the width is relative constant and minimal. Our model predicts for each of these combinations of corridor width and length a gateway depth that could sustain a Mediterranean at gypsum saturation. We do so for the whole set of corridors, to be able to study as many different cases as possible. The calculated depths are indicated in the last column of Table 1.

For the wider and/or shorter corridors (Strait of Gibraltar, southern Rifian, North-Betic Strait) the calculated depth would be of the order of 10 m or less. Such a very shallow depth would cause the basin salinity to move in and out of the gypsum saturation (as discussed in Section 4.3) if the global sea level varies, or might even close the strait, which would lead to falling sea level in the Mediterranean during the PLG, which is not seen in the record (see section 2 for discussion). Narrower or longer gateways (northern Rifian, Guadalhorce, Guadix and Granada) yield a depth up to around 35 m. These depths would permit such sea level variation.

Our model suggests, purely in terms of dimensions and disregarding the proposed ages, that only the northern Rifian, the Guadalhorce, the Guadix and the Granada corridor are corridors of the type that could cause the Mediterranean to reach gypsum saturation during the PLG stage. All these are suggested to have been closed before the PLG stage (last to close is the Guadalhorce corridor around 6.3 Ma (Martín et al.,

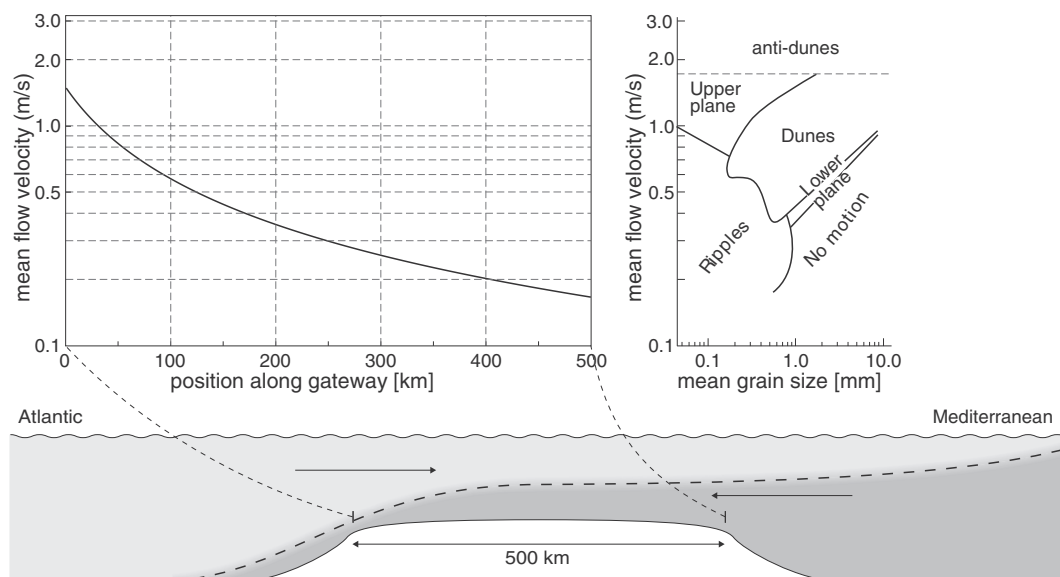


Fig. 9. At the bottom our idealised gateway for a depth of 30 m, a width of 1.5 km and a length of 500 km is shown. The plot on the top left indicates the approximated mean flow velocity (log scale) of the bottom layer, using our model, for the positions along the gateway. This can be easily compared to the simplified bed form phase diagram following Leeder (1999), Boguchwal and Southard (1990) and Ashley et al. (1990) on the top right.

Table 1

Many gateways have been reconstructed for the late Miocene, here is a list of the main ones. They are also indicated on the map of Fig. 1 with the numbers given in the first column. The table shows the approximate width and length from the reconstructions. The last column shows the depths these gateways would need to have in order to cause a Mediterranean at Gypsum saturation, based on our study. The dimensions follow from the studies by Blanc (2002), Wernli (1988), Krijgsman et al. (1999b), Martín et al. (2001), Corbí et al. (2012), Hüsing et al. (2010), Betzler et al. (2006), Martín et al. (2009) and by personal communication with José M. Martín.

Position on Figure 1	Gateway	Width [km]	Length [km]	Estimated Depth (Gypsum) [m]
1	Strait of Gibraltar	13	60	5–11
2	Northern Rifian	10	400	8–17
3	Southern Rifian	50	600	<8
4	Guadalhorce (Betics)	2	100	14–31
5	Granada (Betics)	2	50	15–29
6	Guadix (Betics)	2	50	15–29
7	North-Betic Strait	20	200	<10

2001)). This brings us back to one of the initial question: Where was this gateway located and where can we find the sediments deposited within it? It could be that there existed a corridor of dimensions similar to the ones listed above, that does not appear in the records at all, because it has been removed by erosion, for example due to the opening of the Strait of Gibraltar (García-Castellanos et al., 2009).

6. Conclusions

This study uses the theory of hydraulic control including the effect of bottom friction in order to explore the dimensions of the gateway that must have existed during the PLG phase of the MSC. The results were compared with field observations and constraints on sea level variation locally and globally. This allows us to consider what sedimentary regime is anticipated within the gateway and which of the possible corridors may have been the conduit for exchange during PLG precipitation.

Our main findings are:

1. In order to cause a salinity crisis, the outflux through the gateway needs to be around 25% or less of the influx to reach gypsum saturation and around 10% or less to reach halite saturation.
2. A basin of enhanced salinity relative to its connected ocean needs a negative water budget and a restricted gateway. Restriction, effectively, means a reduction in exchange flux ratio (Q_{out}/Q_{in}), which can be achieved by shallowing, narrowing and/or lengthening of the gateway.
3. The idealised Atlantic–Mediterranean connection that led to the MSC has been approximated, to first order, to a minimum depth of 30–45 m and a maximum width of about 0.7–2 km for a gateway length up to 500 km.
4. Sedimentation is expected in the PLG gateway, with ripples on the Mediterranean side and dunes/anti-dunes on the Atlantic side.
5. The calculated gateway dimensions alone (i.e., disregarding the, as yet, limited geological constraints on the age of closure) would exclude some of the reconstructed late Miocene gateways from being the conduit for exchange during the PLG stage of the MSC. The only gateways that lie in the right dimension region are the northern Rifian, the Guadalhorce, the Guadix and the Granada corridor.

Acknowledgements

We thank Rinus Wortel, Robin Topper and Alba de la Vara, the whole MEDGATE Team and in particular Rachel Flecker for the valuable discussions and insightful comments to this study. We are grateful to two reviewers (José Martín and anonymous) for their valuable comments on the manuscript, and to Michele Rebesco for the editorial handling. Moreover thanks go to C & M Carto for producing Fig. 3 and posting the rest of the figures. The research leading to these results has received funding from the People Programme (Marie Curie Actions) of the

European Unions Seventh Framework Programme FP7/2007–2013/ under REA Grant Agreement No. 290201 MEDGATE.

Appendix A. Detailed theory

A.1. From the conservation of momentum to hydraulic control

How to move from the shallow water equations to the hydraulic equation including bottom friction is laid out here, following Assaf and Hecht (1974); Pratt and Whitehead (2007):

$$u_{out} \frac{du_{out}}{dx} - u_{in} \frac{du_{in}}{dx} = g' \frac{dh_{in}}{dx} + C_D \frac{u_{out}^2}{h_{out}} \quad (A.1)$$

This equation represents the difference in inertia between bottom and top layer on the left hand side and the pressure gradient and friction term on the right hand side, where u_{out}/u_{in} and h_{out}/h_{in} are the average out/inflowing velocity and the average bottom/top layer depth, respectively. g' is the reduced gravity, C_D is the bottom friction coefficient and x represents the direction along the corridor. Now $Q = u * h * w$ is used to transfer from velocities to fluxes, which becomes important later in order to connect to the conservation of salt and water.

$$\frac{Q_{out}^2}{w^2 h_{out}} \frac{d(1/h_{out})}{dx} - \frac{Q_{in}^2}{w^2 h_{in}} \frac{d(1/h_{in})}{dx} = g' \frac{dh_{in}}{dx} + C_D \frac{Q_{out}^2}{w^2 h_{out}^3} \quad (A.2)$$

To simplify the differentials the quotient rule $\frac{dh^{-1}}{dx} = -h^{-2} \frac{dh}{dx}$ is applied:

$$-\frac{Q_{out}^2}{h_{out}^3} \frac{dh_{out}}{dx} + \frac{Q_{in}^2}{h_{in}^3} \frac{dh_{in}}{dx} = w^2 g' \frac{dh_{in}}{dx} + C_D \frac{Q_{out}^2}{h_{out}^3} \quad (A.3)$$

Lawrence (1993) shows that the surface slope along the channel depends on the density difference of the two water layers and on the Froude numbers of the different flows, but is also directly proportional to the channel bottom slope. The channel bottom slope of our channel is zero, therefore the surface slope is also zero. This leads us to the equation $h = h_{in} + h_{out} = \text{constant}$, which allows us to simplify the equation, as it has been done often before (e.g. Assaf and Hecht (1974); Zaremba et al. (2003)), to:

$$\frac{Q_{out}^2}{h_{out}^3} \frac{dh_{in}}{dx} + \frac{Q_{in}^2}{h_{in}^3} \frac{dh_{in}}{dx} = w^2 g' \frac{dh_{in}}{dx} + C_D \frac{Q_{out}^2}{h_{out}^3} \quad (A.4)$$

This can be rearranged to:

$$\frac{dh_{in}}{dx} \left[\frac{Q_{out}^2}{h_{out}^3} + \frac{Q_{in}^2}{h_{in}^3} - w^2 g' \right] = C_D \frac{Q_{out}^2}{h_{out}^3} \quad (A.5)$$

which can be written as:

$$\frac{Q_{in}^2}{h_{in}^3} + \frac{Q_{out}^2}{h_{out}^3} [1 + F] = w^2 g' \quad (A.6)$$

where

$$F = C_D / \frac{dh_{out}}{dx} \quad (A.7)$$

A.2. Connecting the conservation of momentum, salt and water

Combining equations of the conservation of salt and water, the Knudsen relations (Knudsen, 1900; Nielsen, 1908) follow:

$$Q_{in} = \frac{e}{1 - S_A/S_M} \quad (A.8)$$

$$Q_{out} = \frac{e}{S_M/S_A - 1} \quad (A.9)$$

Inserting these into Eq. (A.6), it results in:

$$\frac{e}{(1 - S_A/S_M)^2 (1 - f)^3} + \frac{e}{(S_M/S_A - 1)^2 f^3} (1 + F) = h^3 w^2 \quad (A.10)$$

Where $h_{out} = fh$ and $h_{in} = (1 - f)h$.

This turns into:

$$\frac{1}{(1 - S_A/S_M)^2 (1 - f)^3} + \frac{1 + F}{(S_M/S_A - 1)^2 f^3} = BC * \frac{S_M - S_A}{\rho_A + \beta(S_M - S_A)} \quad (A.11)$$

where

$$BC = \frac{h^3 w^2 g \beta}{e^2} \quad (A.12)$$

Eq. (A.11) is the equation used to plot Fig. A.4, which is used to compute all the results for different gateway settings.

References

- Aharon, P., Goldstein, S.L., Wheeler, C.W., Jacobson, G., 1993. Sea-level events in the South Pacific linked with the Messinian salinity crisis. *Geology* 21, 771–775.
- Anati, D.A., Assaf, G., Thompson, R., 1977. Laboratory models of sea straits. *J. Fluid Mech.* 81, 341–351.
- Armi, L., Farmer, D., 1987. A generalization of the concept of maximal exchange in a strait. *J. Geophys. Res.* 92 (C13), 14679–14680.
- Ashley, G.M., et al., 1990. Classification of large-scale subaqueous bedforms: a new look at an old problem-SEPM bedforms and bedding structures. *J. Sediment. Res.* 60.
- Assaf, G., Hecht, A., 1974. Sea straits: a dynamical model. *Deep Sea Research and Oceanographic Abstracts*. Elsevier, pp. 947–958.
- Betzler, C., Braga, J.C., Martín, J.M., Sánchez-Almazo, I.M., Lindhorst, S., 2006. Closure of a seaway: stratigraphic record and facies (Guadix basin, Southern Spain). *Int. J. Earth Sci.* 95, 903–910.
- Blanc, P.L., 2002. The opening of the Plio-Quaternary Gibraltar Strait: assessing the size of a cataclysm. *Geodin. Acta* 15, 303–317.
- Boguchwal, L.A., Southard, J.B., 1990. Bed configurations in steady unidirectional water flows. Part 1. Scale model study using fine sands. *J. Sediment. Res.* 60.
- Braga, J., Martín, J., 1996. Geometries of reef advance in response to relative sea-level changes in a Messinian (uppermost Miocene) fringing reef (Cariatiz reef, Sorbas basin, SE Spain). *Sediment. Geol.* 107, 61–81.
- Braga, J.C., Martín, J.M., Riding, R., Aguirre, J., Sánchez-Almazo, I.M., Dinarès-Turell, J., 2006. Testing models for the Messinian salinity crisis: the Messinian record in Almería, SE Spain. *Sediment. Geol.* 188, 131–154.
- Bryden, H., Stommel, H., 1984. Limiting processes that determine basic features of the circulation in the Mediterranean Sea. *Oceanol. Acta* 7, 289–296.
- CIESM, 2008. In: Briand, F.E. (Ed.), The messinian salinity crisis from megadeposits to microbiology consensus report. CIESM Workshop Monogr. 33 (168 pp.).
- Corbí, H., Lancis, C., García-García, F., Pina, J.A., Soria, J.M., Tent-Manclús, J.E., Viseras, C., 2012. Updating the marine biostratigraphy of the Granada basin (central betic cordillera): insight for the late Miocene palaeogeographic evolution of the Atlantic-Mediterranean seaway. *Geobios* 45, 249–263.
- Dalziel, S.B., 1992. Maximal exchange in channels with nonrectangular cross sections. *J. Phys. Oceanogr.* 22 (10), 1188–1206.
- de la Vara Fernández, A., Topper, R., Meijer, P., Kouwenhoven, T., 2015. Water exchange through the Betic and Rifian corridors prior to the Messinian salinity crisis: a model study. (in review).
- Farmer, D.M., Armi, L., 1986. Maximal two-layer exchange over a sill and through the combination of a sill and contraction with barotropic flow.
- Farmer, D.M., Armi, L., 1988. The flow of Atlantic water through the Strait of Gibraltar.
- Feistel, R., 2008. A Gibbs function for seawater thermodynamics for -6 to 80 Å° c and salinity up to 120 g kg⁻¹. *Deep-Sea Res. I Oceanogr. Res. Pap.* 55, 1639–1671.
- Flecker, R., the MEDGATE Team, 2015. Late Miocene Evolution of the Mediterranean-Atlantic Gateways (in preparation).
- García-Veigas, J., Cendón, D.I., Rosell, L., Ort, F., Torres Ruiz, J., Martín, J.M., Sanz, E., 2013. Salt deposition and brine evolution in the Granada basin (late Tortonian, SE Spain). *Palaeogeogr. Palaeoclimatol. Palaeoecol.* 369, 452–465.
- García-Veigas, J., Rosell, L., Cendón, D.I., Gibert, L., Martín, J.M., Torres-Ruiz, J., Ort, F., 2015. Large celestine orebodies formed by early-diagenetic replacement of gypsified stromatolites (upper Miocene, Monteive-Escúzar deposit, Granada basin, Spain). *Ore Geol. Rev.* 64, 187–199.
- García-Castellanos, D., Estrada, F., Jiménez-Munt, I., Gorini, C., Fernández, M., Vergés, J., De Vicente, R., 2009. Catastrophic flood of the Mediterranean after the Messinian salinity crisis. *Nature* 462, 778–781.
- Garrett, C., 2004. Frictional processes in straits. *Deep-Sea Res. II Top. Stud. Oceanogr.* 51, 393–410.
- Gladstone, R., Flecker, R., Valdes, P., Lunt, D., Markwick, P., 2007. The Mediterranean hydrologic budget from a late Miocene global climate simulation. *Palaeogeogr. Palaeoclimatol. Palaeoecol.* 251, 254–267.
- Gu, L., Lawrence, G.A., 2001. Frictional exchange flow through a ship canal. *Proceedings of the Congress-International Association for Hydraulic Research*, pp. 433–438.
- Gu, L., Lawrence, G.A., 2005. Analytical solution for maximal frictional two-layer exchange flow. *J. Fluid Mech.* 543, 1–17.
- Hilgen, F., 1991. Extension of the astronomically calibrated (polarity) time scale to the Miocene/Pliocene boundary. *Earth Planet. Sci. Lett.* 107, 349–368.
- Hilgen, F., Kuiper, K., Krijgsman, W., Snel, E., van der Laan, E., 2007. Astronomical tuning as the basis for high resolution chronostratigraphy: the intricate history of the Messinian salinity crisis. *Stratigraphy* 4, 231–238.
- Hodell, D.A., Curtis, J.H., Sierro, F.J., Raymo, M.E., 2001. Correlation of late Miocene to early Pliocene sequences between the Mediterranean and North Atlantic. *Paleoceanography* 16, 164–178.
- Hsü, K., Ryan, W., Cita, M., et al., 1973. Late Miocene desiccation of the Mediterranean. *Nature* 242, 240–244.
- Hüsing, S., Oms, O., Agust, J., Garcés, M., Kouwenhoven, T., Krijgsman, W., Zachariasse, W.J., 2010. On the late Miocene closure of the Mediterranean-Atlantic gateway through the Guadix basin (southern Spain). *Palaeogeogr. Palaeoclimatol. Palaeoecol.* 291, 167–179.
- Ivanovic, R.F., Flecker, R., Gutjahr, M., Valdes, P.J., 2013. First Nd isotope record of Mediterranean-Atlantic water exchange through the Moroccan Rifian Corridor during the Messinian salinity crisis. *Earth Planet. Sci. Lett.* 368, 163–174.
- Ivey, G.N., 2004. Stratification and mixing in sea straits. *Deep Sea Research Part II: Topical Studies in Oceanography* 51 (4), 441–453.
- Johns, W., Yao, F., Olson, D., Josey, S., Grist, J., Smeed, D., 2003. Observations of seasonal exchange through the Straits of Hormuz and the inferred heat and freshwater budgets of the Persian Gulf. *J. Geophys. Res. Oceans* 108, 108.
- Knudsen, M., 1900. Ein hydrographischer Lehrsatz. *Annalen der Hydrographie und Maritimen Meteorologie* 28 (7), 316–320.
- Kostachuk, R., Villard, P., 1996. Flow and sediment transport over large subaqueous dunes: Fraser River, Canada. *Sedimentology* 43, 849–863.
- Krijgsman, W., Hilgen, F., Raffi, I., Sierro, F., Wilson, D., 1999a. Chronology, causes and progression of the Messinian salinity crisis. *Nature* 400, 652–655.
- Krijgsman, W., Langereis, C., Zachariasse, W., Boccaletti, M., Moratti, G., Gelati, R., Iaccarino, S., Papani, G., Villa, G., 1999b. Late Neogene evolution of the Taza-Guercif Basin (Rifian Corridor, Morocco) and implications for the Messinian salinity crisis. *Mar. Geol.* 153, 147–160.
- Krijgsman, W., Fortuin, A., Hilgen, F., Sierro, F., 2001. Astrochronology for the Messinian Sorbas basin (SE Spain) and orbital (precessional) forcing for evaporite cyclicity. *Sediment. Geol.* 140, 43–60.
- Lawrence, G.A., 1993. The hydraulics of steady two-layer flow over a fixed obstacle. *Journal of Fluid Mechanics* 254, 605–633.
- Leeder, M., 1999. *Sedimentology and Sedimentary Basins: From Turbulence to Tectonics*. Wiley-Blackwell.
- Lofi, J., Déverchère, J., Gaullier, V., Gillet, H., Gorini, C., Guennoc, P., Loncke, L., Maillard, A., Sage, F., Thion, I., et al., 2011. Seismic atlas of the Messinian salinity crisis markers in the Mediterranean and black seas. *Mem. Soc. Géol. n.s.* 179, 1–72.
- Lugli, S., Manzi, V., Roveri, M., 2008. New facies interpretation of the Messinian evaporites in the Mediterranean. CIESM Workshop, Monogr. pp. 67–72.
- Lugli, S., Manzi, V., Roveri, M., Schreiber, C., 2010. The Primary Lower Gypsum in the Mediterranean: a new facies interpretation for the first stage of the Messinian salinity crisis. *Palaeogeogr. Palaeoclimatol. Palaeoecol.* 297, 83–99.
- Manzi, V., Gennari, R., Hilgen, F., Krijgsman, W., Lugli, S., Roveri, M., Sierro, F.J., 2013. Age refinement of the Messinian salinity crisis onset in the Mediterranean. *Terra Nova* 25 (4), 315–322.
- Mariotti, A., Struglia, M.V., Zeng, N., Lau, K., 2002. The hydrological cycle in the Mediterranean region and implications for the water budget of the Mediterranean Sea. *J. Clim.* 15, 1674–1690.
- Martín, J., Ortega-Huertas, M., Torres-Ruiz, J., 1984. Genesis and evolution of strontium deposits of the Granada basin (southeastern Spain): evidence of diagenetic replacement of a stromatolite belt. *Sediment. Geol.* 39, 281–298.

- Martín, J.M., Braga, J.C., Betzler, C., 2001. The Messinian Guadalhorce corridor: the last northern, Atlantic–Mediterranean gateway. *Terra Nova* 13, 418–424.
- Martín, J.M., Braga, J.C., Aguirre, J., Puga-Bernabéu, Á., 2009. History and evolution of the North-Betic Strait (Prebetic Zone, Betic Cordillera): a narrow, early Tortonian, tidal-dominated, Atlantic–Mediterranean marine passage. *Sediment. Geol.* 216, 80–90.
- Martín, J.M., Puga-Bernabéu, Á., Aguirre, J., Braga, J.C., 2014. Miocene Atlantic–Mediterranean seaways in the Betic Cordillera (Southern Spain). *Rev. Soc. Geol. Esp.* 27, 1.
- Meijer, P., 2012. Hydraulic theory of sea straits applied to the onset of the Messinian salinity crisis. *Mar. Geol.* 326, 131–139.
- Meijer, P., Krijgsman, W., 2005. A quantitative analysis of the desiccation and re-filling of the Mediterranean during the Messinian salinity crisis. *Earth Planet. Sci. Lett.* 240, 510–520.
- Nielsen, J.N., Hydrography of the Mediterranean and adjacent waters
- Officer, C., et al., 1976. *Physical Oceanography of Estuaries (and Associated Coastal Waters)*.
- Özsoy, E., Di Iorio, D., Gregg, M.C., Backhaus, J.O., 2001. Mixing in the Bosphorus Strait and the Black Sea continental shelf: observations and a model of the dense water outflow. *Jour. Marine Sys.* 31 (1), 99–135.
- Pérez-Asensio, J., Aguirre, J., Schmiedl, G., Civis, J., 2012. Impact of restriction of the Atlantic–Mediterranean gateway on the Mediterranean outflow water and eastern Atlantic circulation during the Messinian. *Paleoceanography* 27.
- Pratt, L., 1984. A time-dependent aspect of hydraulic control in straits. *J. Phys. Oceanogr.* 14, 1414–1418.
- Pratt, L., 1986. Hydraulic control of sill flow with bottom friction. *J. Phys. Oceanogr.* 16, 1970–1980.
- Pratt, L., Whitehead, J., 2007. *Rotating hydraulics: Nonlinear topographic effects in the ocean and atmosphere* vol. 36. Springer.
- Rohling, E., Schiebel, R., Siddall, M., 2008. Controls on Messinian lower evaporite cycles in the Mediterranean. *Earth Planet. Sci. Lett.* 275, 165–171.
- Roveri, M., Flecker, R., Krijgsman, W., Lofi, J., Lugli, S., Manzi, V., Sierro, F.J., Bertini, A., Camerlenghi, A., De Lange, G., et al., 2014. The Messinian salinity crisis: past and future of a great challenge for marine sciences. *Mar. Geol.* 352, 25–58.
- Santisteban, C., Taberner, C., 1983. Shallow marine and continental conglomerates derived from coral reef complexes after desiccation of a deep marine basin: the Tortonian–Messinian deposits of the Fortuna basin, SE Spain. *J. Geol. Soc.* 140, 401–411.
- Sofianos, S., Johns, W., Murray, S., 2002. Heat and freshwater budgets in the Red Sea from direct observations at Bab el Mandeb. *Deep-Sea Res. II Top. Stud. Oceanogr.* 49, 1323–1340.
- Stommel, H., Farmer, H., 1953. Control of salinity in an estuary by a transition. *J. Mar. Res.* 12, 13–20.
- Te Chow, V., 1959. *Open Channel Hydraulics*. McGraw-Hill Book Company, Inc, New York.
- Topper, R., Flecker, R., Meijer, P.T., Wortel, M., 2011. A box model of the late Miocene Mediterranean Sea: implications from combined 87Sr/86Sr and salinity data. *Paleoceanography* 26, PA3223.
- Tsimplis, M., Zervakis, V., Josey, S.A., Peneva, E., Struglia, M.V., Stanev, E., Lionello, P., Malanotte-Rizzoli, P., Artale, V., Theocharis, A., et al., 2006. *Changes in the Oceanography of the Mediterranean Sea and Their Link to Climate Variability*.
- Warren, J.K., 2006. *Evaporites: Sediments, Resources and Hydrocarbons: Sediments, Resources, and Hydrocarbons*. Springer.
- Wernli, R., 1988. Micropaleontology of the Neogene nappes du Maroc septentrional et description systématique des foraminifères planctoniques. *Notes Mem. Serv. Geol. Maroc* 331.
- Whitehead, J., 1998. Topographic control of oceanic flows in deep passages and straits. *Rev. Geophys.* 36, 423.
- Zaremba, L.J., Lawrence, G., Pieters, R., 2003. Frictional two-layer exchange flow. *J. Fluid Mech.* 474, 339–354.
- Zhu, D.Z., Lawrence, G.A., 2000. Hydraulics of exchange flows. *J. Hydraul. Eng.* 126, 921–928.